Journal of Biomolecular NMR (2006) 35: 249–259
DOI 10.1007/s10858-006-9037-6

Article

Determination of the residue-specific ^{15}N CSA tensor principal components using multiple alignment media

Robert A. Burton & Nico Tjandra*
Laboratory of Molecular Biophysics, National Heart, Lung, and Blood Institute, National Institutes of Health, 50 South Drive, Bethesda, Maryland, 20892, USA

Received 23 February 2006; Accepted 2 June 2006

Key words: alignment, chemical shift anisotropy, chemical shift tensor, NMR, residual dipolar couplings

Abstract

The individual components of the backbone ^{15}N CSA tensor, σ_{11}, σ_{22}, σ_{33}, and the orientation of σ_{11} relative to the NH bond described by the angle β have been determined for uniformly labeled ^{15}N, ^{13}C ubiquitin from partial alignment in phospholipid bicelles, Pf1 phage, and poly(ethylene glycol) by measuring the residue-specific residual dipolar couplings and chemical shift deviations. No strong correlation between any of the CSA tensor components is observed with any single structural feature. However, the experimentally determined tensor components agree with the previously determined average CSA principal components [Cornilescu and Bax (2000) *J. Am. Chem. Soc.* **122**, 10143–10154]. Significant deviations from the averages coincide with residues in β-strand or extended regions, while α-helical residue tensor components cluster close to the average values.

Introduction

Knowledge of the chemical shift anisotropy (CSA) tensor is integral to the quantitative determination and understanding of dynamics and relaxation rates (Fischer et al., 1998a; Fischer et al., 1998b; Lienin et al., 1998; Scheurer et al., 1999), cross-correlation and relaxation interference (Pervushin et al., 1997; Reif et al., 1997; Brutscher et al., 1998; Reif et al., 1998; Yang and Kay, 1998; Salzmann et al., 1999; Yang and Kay, 1999; Chiarparin et al., 2000), and NMR structure determination (Mai et al., 1993; Ketchem et al., 1996; Feng et al., 1997; Marassi and Opella, 1998; Long and Tycko, 1998; Marassi et al., 1999; Fu and Cross, 1999; Ishii and Tycko, 2000; Lipsitz and Tjandra, 2001). Traditionally, it has been difficult to determine and interpret ^{15}N CSA data from liquid state NMR because they could only be deduced from relaxation-based measurements. This requires extremely accurate measurements of various relaxation rates, separation of the CSA contribution from the total rate, and separation of the CSA and order parameters. Protein partial alignment in solution affords the measurement of residual dipolar coupling (D_{NH}) and differences in chemical shift ($\Delta\delta$). It is, however, not trivial to obtain a meaningful analysis of the ^{15}N CSA because it requires the measurement of tiny perturbations (tens of ppb) observed in the chemical shift resulting from reintroduction of the CSA tensor due to partial alignment. Also, it has been known for quite some time that the chemical shifts of backbone nitrogen atoms are exquisitely sensitive to nearby backbone and side-chain geometry, hydrogen bonding, solvent effects such as pH and ionic strength, and nearest neighbor effects (Braun et al., 1994; Le and Oldfield, 1994; Oldfield, 1995;

*To whom correspondence should be addressed. E-mail: tjandran@nhlbi.nih.gov

Palmer et al., 1996; Tjandra and Bax, 1997; Case, 1998; Sitkoff and Case, 1998; Cornilescu et al., 1999; Xu and Case, 2002). This sensitivity can be potentially useful in providing unique structural as well as dynamic information. However, because of the complexity of the interactions, it has proven difficult to isolate the cause and effect relationships of each individual contributor to the overall ^{15}N CSA or to the magnitude and orientation of the individual tensor components. Density functional theory (DFT) calculations have revealed that both torsion angles and hydrogen bonding have a profound effect on the ^{15}N isotropic chemical shift (Xu and Case, 2002) leading to shifts of up to 6–8 ppm. Contributions from nearest neighbors and side-chain χ angles are equally significant. Interestingly, it was shown that indirect hydrogen bonds (to the carbonyl of the peptide) had a more significant impact on ^{15}N isotropic shift than direct hydrogen bonding. Other atoms, such as C^{α}, C^{β}, and H^{α}, are not as sensitive to these factors and have thus far proven more useful for qualitative comparisons between secondary structure and chemical shift (Wishart et al., 1992; Wishart and Sykes, 1994).

The average values for the ^{15}N CSA tensor components have recently been experimentally determined under the assumption that all atoms of the same type have the same tensor (Cornilescu and Bax, 2000). However, previous experimental data suggest high variability in the ^{15}N CSA tensor as deduced from the projection of the CSA tensor components, $\sigma_{\parallel}$ and $\sigma_{\perp}$, for individual residues using the cross correlation and transverse relaxation rates (Fushman et al., 1998; Kroenke et al., 1999). Despite these previous efforts, the residue-specific individual components of the CSA tensor have not been heretofore reported.

We have used multiple alignment media, including phospholipid bicelles, Pf1 phage, and 8% poly(ethylene glycol), to obtain both the residual dipolar coupling data (D_{NH}) as well as the chemical shift differences ($\Delta\delta_N$) of individual ^{15}N backbone atoms. The D_{NH} was used to obtain the alignment tensor for each medium. From this information and the three sets of $\Delta\delta_N$, we were able to mathematically solve for the principal components of the ^{15}N CSA tensor (σ_{11}, σ_{22}, σ_{33}) as well as the angle β that describes the relative orientation of σ_{11} to the NH bond. Notwithstanding the error introduced into the measurement by structural noise, solvent effects, and possible interaction with the alignment medium, we were able to produce these data with reasonable precision.

Because of the extreme sensitivity of the ^{15}N nucleus and the many contributors to the ^{15}N chemical shift tensor, it is clear that one cannot expect to find a strong correlation of any individual component of the tensor with any one factor and indeed only weak or no significant correlation was found.

Materials and methods

Sample preparation

Uniformly enriched ^{13}C, ^{15}N purified ubiquitin was dissolved in each of the following buffers at 0.7 mM concentration. Isotropic and anisotropic samples were prepared under identical conditions with the exception of the added liquid crystal phase inducing compounds. Samples for alignment by phage were prepared with 10 mM KPO_4 pH 6.5, 100 mM NaCl and 10% D_2O. Approximately 15 mg/ml of Pf1 phage (Asla biotec) was added to the solution to induce alignment. Samples containing 0–8% cetylpyridinium bromide (CPBR)/hexanol were prepared as previously described (Barrientos et al., 2000) in 50 mM NaOAc pH 5.0, 25 mM NaBr, and 10% D_2O. Samples of 0–8% strained acrylamide gel (SAG) were prepared as described previously (Ishii et al., 2001) in 50 mM NaOAc pH 5.0 and 10% D_2O. Samples containing 0–8% $C_{12}E_5$ poly(ethylene glycol) (PEG)/hexanol were also prepared as described previously. (Ruckert and Otting, 2000) in 50 mM NaOAc pH 5.0 and10% D_2O.

NMR spectra

All NMR spectra were recorded at 298 K on a Bruker Avance-800 spectrometer with 2048×360 complex data points zero filled to 4096×4096 and 2048 dummy scans to ensure temperature stabilization. Acquisition times were 221.8 ms in the t_1 dimension and 106.6 ms in the t_2 dimension. All PEG/hexanol and CPBR/hexanol containing samples were allowed to align in the magnetic field for 6–12 h before recording spectra. ^{1}H–^{15}N HSQC with and without ^{1}H–^{15}N decoupling and IPAP-HSQC spectra. (Ottiger et al., 1998) were

recorded in the absence and presence of liquid crystal phase inducing components. All data were processed with NMRPipe (Delaglio et al., 1995). Peaks were picked and contour selected/averaged with PIPP (Garrett et al., 1991).

Results and discussion

Measurement of D_{NH} and $\Delta\delta_N$

D_{NH} values for uniformly ^{13}C, ^{15}N labeled ubiquitin were determined by calculating the difference between the observed backbone $J_N - HN$ of the isotropic and anisotropic data sets obtained from the $^{1}H–^{15}N$ HSQC/IPAP-HSQC experiments. These data were fit to the high-resolution ubiquitin NMR structure (Cornilescu et al., 1998) by minimizing the difference between the experimental and calculated D_{NH} values (de Alba and Tjandra, 2002; Prestegard et al., 2004; Bax and Grishaev, 2005) and the results are compiled in Table 1.

The $\Delta\delta_N$ were measured by peak picking only contour averaged peaks that were separated at half-height and of sufficient intensity to yield several contours in both the isotropic and anisotropic $^{1}H–^{15}N$ HSQC spectra. Predicted D_{NH} and $\Delta\delta_N$ values for the bicelle, phage, and PEG data sets were calculated from the appropriately rotated high-resolution NMR structure (Cornilescu et al., 1998) using the previously reported average values for $\sigma_{11} = -108.5$ ppm, $\sigma_{22} = 45.7$ ppm, $\sigma_{33} = 62.8$ ppm, and $\beta = 19°$.

As can be seen in Figure 1, the measured $\Delta\delta_N$ from the various alignment phases range from approximately −100 to 100 ppb in phage (average = 11.7 ± 51 ppb), which has the weakest alignment, to −150 to 200 ppb for 8% PEG/hexanol (average = −37.3 ± 88 ppb), which has the strongest alignment. The reproducibility error in the measured $\Delta\delta_N$ for the phage and PEG/hexanol systems is 2.4 and 2.5 ppb respectively.

The D_{NH} and $\Delta\delta_N$ data for ubiquitin in phospholipid bicelles were obtained from the previously published work of Cornilescu and Bax. (Cornilescu and Bax, 2000). Information regarding the molecular alignment tensor for ubiquitin in bicelles is also contained in Table 1. The alignment tensors are mostly independent except that bicelles and PEG have a similar tensor direction. However, the rhombicities for these two tensors are quite different and thus can still be regarded as independent probes for the $\Delta\delta_N$.

The expected residual CSA values can be calculated by creating the tensorial projection of the chemical shift tensor onto the molecular alignment frame as described in the equation for $\Delta\delta_N$:

$$\Delta\delta_N = \sum_{i=x,y,z} \sum_{j=x,y,z} A_{jj} \cos^2 \theta_{ij} \sigma_{ii} \quad (1)$$

where A_{jj} is the magnitude of the alignment tensor in the x, y, and z, directions, and θ is the angle between the traceless principal axes of the molecular alignment tensor, A_{jj}, and the CSA tensor, σ_{ii}. The alignment tensor used in the calculation of $\Delta\delta_N$ was derived from fitting the D_{NH} data.

The correlation between the calculated and experimental D_{NH} and $\Delta\delta_N$ data obtained from the Pf1 phage and 8% PEG/hexanol data sets is shown in Figure 2. Experimental data have been

Table 1. Orientation and magnitude of the alignment tensor for ubiquitin in various liquid crystalline phases[a]

	Bicelles	Pf1 phage	8% PEG
α(°)	28	50	17
β(°)	32	144	28
γ(°)	24	49	35
Da (Hz)	12.7	9.2	−18.5
R	0.61	0.52	0.17
$10^4\ A_{xx}$	0.33	−0.62	4.90
$10^4\ A_{yy}$	7.47	−5.02	7.54
$10^4\ A_{zz}$	−7.80	5.64	−12.44

[a] α, β, and γ, are the Euler angles defining the alignment tensor relative to the coordinate frame of the high resolution NMR structure following the convention of successive rotations about z, y, z. A_{xx}, A_{yy}, and A_{zz} are the magnitudes of the principal components of the alignment tensor. The correlation r-factor is −0.5 between D_{NH} obtained for bicelles and phage, −0.8 between bicelles and PEG, and 0.2 for phage and PEG.

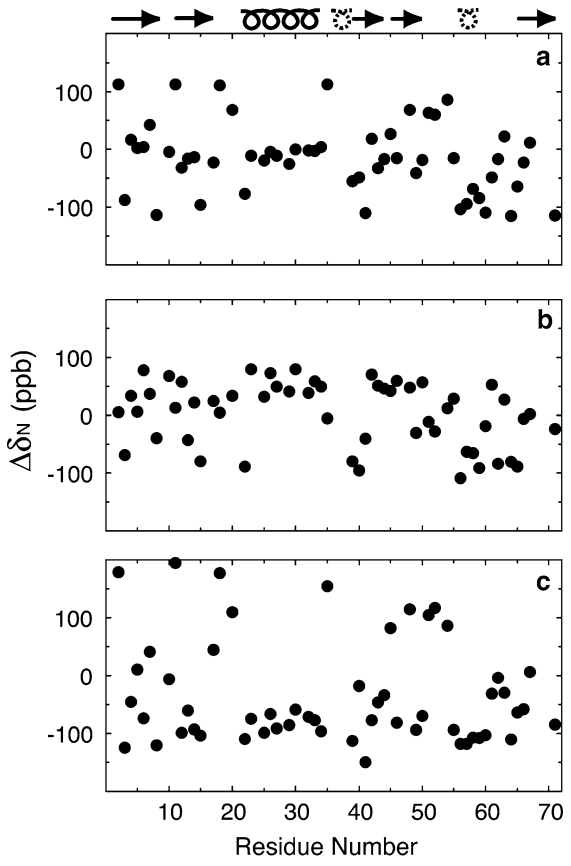

Figure 1. Experimental $\Delta\delta_N$ for ubiquitin under alignment induced by bicelles (a), Pf1 phage (b), and 8% PEG/hexanol (c). The calculated error for $\Delta\delta_N$ between successive identical experiments is 2.5 ppb for samples aligned with PEG/hexanol and 2.4 ppb for samples aligned with phage. The secondary structural elements as determined by the program MOLMOL (Koradi et al., 1996) are represented above panel (a). Arrows represent β-strands, coils represent α-helices. A dotted coil indicates a 3_{10}-helix.

corrected for lock shift (D_2O doublet due to alignment) and solvent effect where necessary. Additionally, overlapped or weak signals have been removed. See Supplementary Material for a full listing of the residue specific data. Panels a and b of Figure 2 show the correlation between the calculated and experimental D_{NH} and $\Delta\delta_N$ for phage data with an rmsd of 2.2 Hz and 21.5 ppb respectively. Panels c and d show the correlation between the calculated and experimental D_{NH} and $\Delta\delta_N$ for 8% PEG/hexanol data with an rmsd of 3.3 Hz and 19.5 ppb respectively. All residues undergoing conformational exchange or large amplitude fast internal motions were identified previously (Tjandra et al., 1995). Removal of these residues decreases the respective rmsds to 1.8 Hz, 19.0 ppb, 3.1 Hz, and 18.7 ppb for panels a, b, c, and d. Following the same protocol with the previously reported ubiquitin data under alignment with bicelles yielded D_{NH} and $\Delta\delta_N$ rmsd values of 1.1 Hz and 14.8 ppb respectively.

Not all data sets are depicted in Figure 2 because not all experimental conditions initially studied produced acceptable correlations between experimental and calculated data sets. The rmsd for the correlation between $\Delta\delta_N$(meas) and $\Delta\delta_N$(calc) for the CPBR/hexanol and SAG data sets was 95.3 and 37.3 ppb respectively and were therefore not used in this study. It is believed that interaction with the alignment material or slight solubility of the alignment compounds in the buffer, thus creating possible small perturbations in structure or inducing a solvent effect, are likely sources of spurious chemical shift deviations. Indeed, the effect of solvent can be seen in the plot of the D_{NH} and $\Delta\delta_N$ at increasing concentrations of PEG/hexanol (Figure 3). No alignment was detected by deuterium splitting or measurable D_{NH} at 1% concentration. However, changes in chemical shifts from the isotropic sample could be measured at this concentration. These shifts must be due to solvent effect created by the PEG/hexanol mixture. As can be seen in Figure 3, the alteration in linear trend at 1% is apparent. The average chemical shift change was 5.9 ± 20.1 ppb indicating that the average solvent effect is small, but some residues are affected to a much larger extent. The degree of solvent exposure most likely exacerbates the observed effect. In order to take into account the shifts due to solvent effect, we corrected the 8% PEG/hexanol data by using the $\Delta\delta_N$ calculated between 0% and 1% PEG/hexanol as an offset. Application of the 0–1% correction factor reduced the rmsd between $\Delta\delta_N$(meas) and $\Delta\delta_N$(calc) from 37.8 to 18.7 ppb.

We were unable to correct for probable solvent effects in the case of alignment by strained acrylamide gel or CPBR/hexanol. No RDCs were observable in unstrained 3% acrylamide gel. However correction of aligned $\Delta\delta_N$ with unstrained 3% $\Delta\delta_N$ values did not improve the correlation between observed and calculated data (data not shown). The samples composed of CPBR/hexanol separated into phases even at low concentrations (1%) and prevented chemical shift measurement without inducing alignment. Such

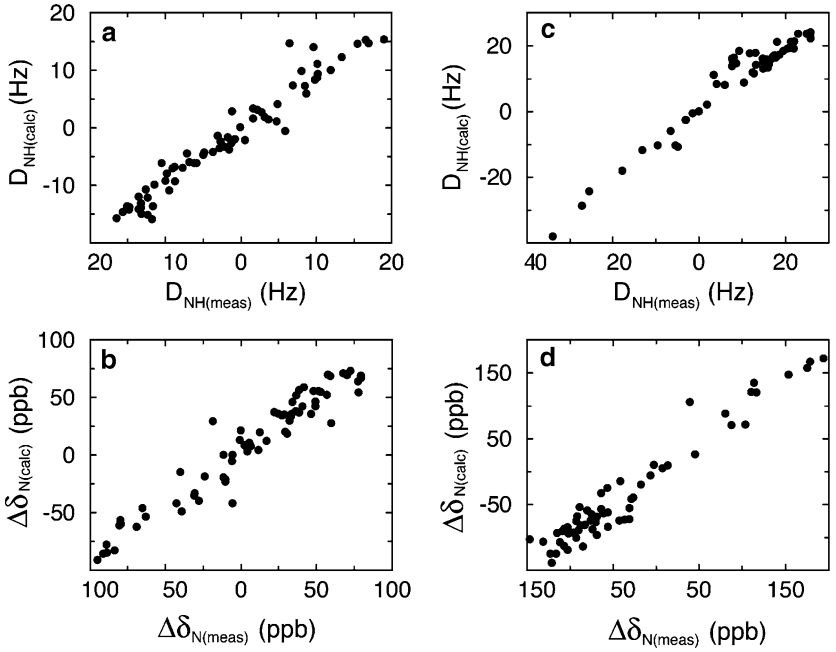

Figure 2. Correlation between D_{NH}(meas) and D_{NH}(calc) (a,c) and $\Delta\delta_N$(meas) and $\Delta\delta_N$(calc) (b,d) for the Pf1 phage (a,b) and 8% PEG/hexanol data sets (c,d).

solvent effects on chemical shift may be present in the other aligned samples, although greatly abrogated. Pf1 phage has no organic solvent component and NaCl is commonly added to prevent electrostatic protein-phage interactions. Alignment in bicelles is induced by an increase in temperature not by alteration of the buffer conditions and corrections in chemical shift due to temperature changes were taken into account in the previously published bicelle data (Cornilescu and Bax, 2000).

Calculation of tensor components

It is important that we initially evaluate whether our new data sets are compatible with the previously published bicelle data by examining the average CSA tensor values calculated independently from the phage and PEG/hexanol alignment media. The averages are determined by numerical minimization of the difference between measured and calculated $\Delta\delta_N$ values, while varying the magnitudes of the CSA tensor. The orientation of the tensor was kept fixed to the values that were published previously for alignment in bicelles. The calculated averages for σ_{11} (-115.9 ± 0.7 ppm, phage; -116.0 ± 0.3 ppm, PEG/hexanol), σ_{22} (42.7 ± 0.6 ppm, phage; 45.0 ± 0.2 ppm for PEG/hexanol), and σ_{33} (65.3 ± 0.4 ppm, phage; 63.2 ± 0.1 ppm, PEG/hexanol) values for our data sets are within a few ppm of the averages published previously (-108.5 ± 3 ppm, 45.7 ± 2 ppm, and 62.8 ± 2 ppm for σ_{11}, σ_{22}, and σ_{33}, respectively) (Cornilescu and Bax, 2000). This agreement confirms the reliability of our experimental data. In fact, considering that the sample conditions and experimental temperatures are very different, it is quite remarkable that one can obtain consistent average values.

The ideal description of the full CSA tensor requires the five parameters σ_{11}, σ_{22}, α, β, and γ where σ_{33} can be derived from the traceless relationship. The number of necessary variables for an approximate solution can be reduced by the observation that σ_{22} is typically normal to the peptide plane and therefore the angles α and γ can be treated as fixed (Harbison et al., 1984; Hartzell et al., 1987; Oas et al., 1987; Hiyama et al., 1988; Lumsden et al., 1994). We were unable to obtain accurate data in four or five alignment media (see discussion above); therefore α and γ were fixed. Taking these restrictions into account leaves three unknowns in the equation. By determining the $\Delta\delta_N$ for individual ubiquitin residues under three

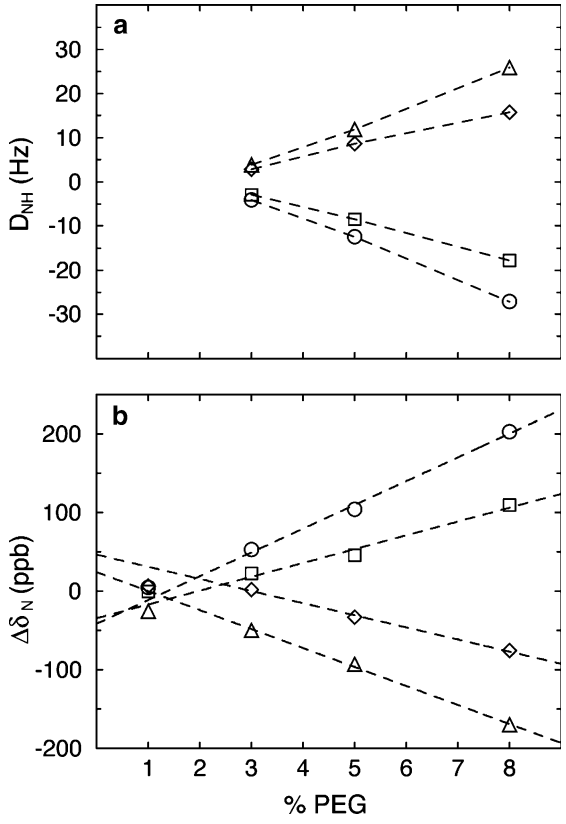

Figure 3. Dependence of D_{NH} (a) and $\Delta\delta_N$ (b) on percent concentration of PEG/hexanol for residues K11 (circle), S20 (square), I23 (diamond), and Q41 (upward triangle). Panel (a) does not show the point of 0 D_{NH} at 1% because it is not known at which percent of PEG/hexanol, between 1 and 3, the D_{NH} actually begins to form, only that at 1% the D_{NH} is 0. Dashed lines in panel b were calculated as a linear regression of only the points at 3, 5, and 8% to show the deviation of the 1% data from the trend.

different alignment conditions we were able to calculate σ_{11}, σ_{22}, σ_{33} and the angle β on a per residue basis (Figure 4).

The ensuing system of equations is non-linear as a function of β and calculation of an analytical solution is quite involved. Therefore, we adopted a numerical protocol to minimize the function $|(\Delta\delta_N(\text{meas}) - \Delta\delta_N(\text{calc}))/\text{error}|$ by varying σ_{11}, σ_{22}, and β with the error estimated from the reproducibility of $\Delta\delta_N$(meas). Figure 4 shows the resultant σ_{11}, σ_{22}, σ_{33}, and β values. The uncertainties in the reported values are represented by the error bars in Figure 4 and were determined from 40 simulated Monte–Carlo data sets generated by adding random Gaussian noise, representative of the error, to $\Delta\delta_N$(meas). Each new data set was then refit to yield the new σ_{11}, σ_{22}, σ_{33}, and β incorporating the error. The uncertainties in the average values (reported below) were also determined in this fashion. As can be seen, only residues that are close to the -NH_2 or -COOH termini, or those that lie far from the average have large error. Excluding these residues, the errors in the principal components of the ^{15}N CSA tensor typically fall within 3%. Interestingly, the regions that show the highest variability coincide with β-strand or extended regions, while the residues located in the α-helix (23–33) generally cluster more closely to the previously determined averages with only residue I30 as an exception. Further analysis of residue I30 revealed that the cosine of the tensorial projection of this residue was distinct from other residues in the central α-helix. Scatter about the average is also greater at the termini versus the interior of the protein. This scatter is most likely due to slight structural variations at the less ordered termini. The standard deviations for σ_{11}, σ_{22}, σ_{33}, and β are 13.0 ppm, 10.6 ppm, 7.0 ppm, and 5.3° for helical segments and 50.3 ppm, 28.5 ppm, 47.4 ppm, and 17.6° respectively for β-strand or extended segments. Furthermore, overall rmsd fluctuation about the σ_{22} average (39.7 ppm) is less than that of σ_{11} (45.6 ppm), implying that there is slightly less of an effect on this component of the ^{15}N CSA tensor than the others.

Propagation of error

The scatter of the data in the correlation plots (Figure 2) and in the principal components of the CSA tensor (Figure 4) behooves a discussion of the error propagation in the measurement and calculations described herein. The experimental error in $\Delta\delta_N$(meas) (2.4 and 2.5 ppb; phage and PEG/hexanol respectively) is significantly smaller than the rmsd of 19.0 and 18.7 ppb between the respective $\Delta\delta_N$(meas) and $\Delta\delta_N$(calc) for the phage and PEG/hexanol systems. Additionally, the Monte–Carlo generated error in $\Delta\delta_N$(meas), σ_{11}, σ_{22}, and β is generally small. Therefore, the data can be meaningfully analyzed, and observed trends and deviations can be considered real. These differences between $\Delta\delta_N$(meas) and $\Delta\delta_N$(calc) must arise from residual solvent effect, small variations in the atomic coordinates, differences in dynamics at specific sites, or actual differences in the CSA tensor. In an attempt to understand how each of

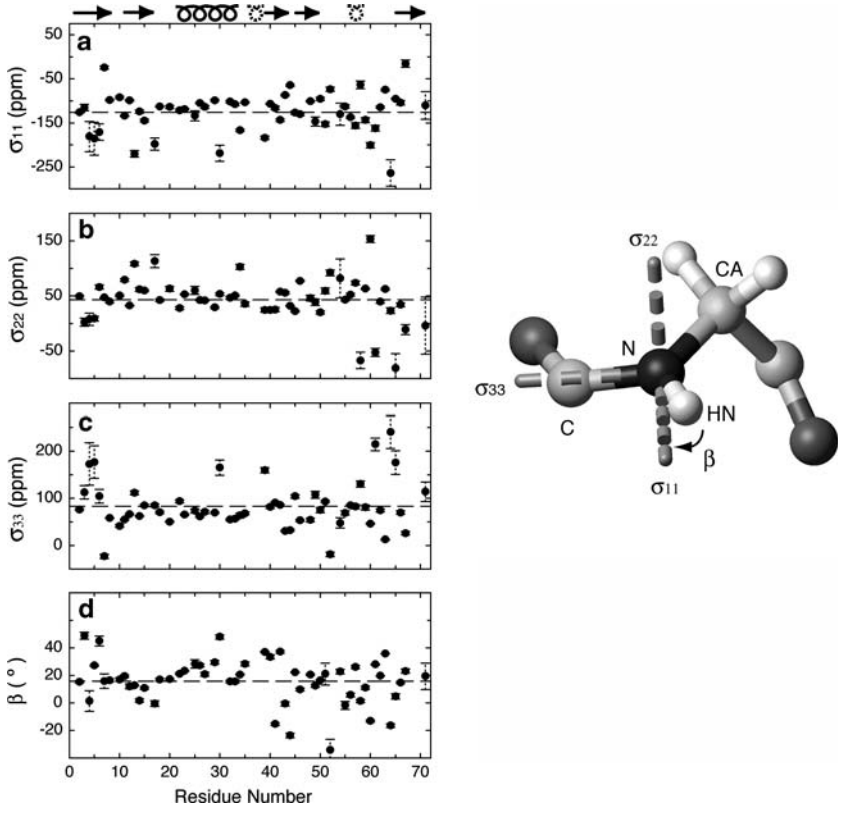

Figure 4. Plot of experimentally determined σ_{11} (a), σ_{22} (b), σ_{33} (c), and β (d). Error bars are derived from the error introduced by 40 Monte–Carlo calculations and the secondary structure elements are shown above. A schematic diagram of the ^{15}N CSA tensor depicting the principal components σ_{11}, σ_{22}, σ_{33} and the Euler angle β is also illustrated by MOLMOL (Koradi et al., 1996).

these factors may be influencing the ^{15}N CSA tensor principal components, we discuss each of these possible effects individually below.

Solvent effect

Most liquid crystal systems used for alignment in NMR require additional compounds to induce phase transition and even slight differences in buffer composition can give rise to changes in $\Delta\delta_N$(meas). Phospholipid bicelles are unique in this aspect in that phase transition is induced by temperature changes, and deviations in $\Delta\delta_N$(meas) as a result of temperature can be corrected using a linear correction factor. Solvent effects, however, may vary widely from residue to residue and therefore must be corrected on a residue-specific basis. Despite the use of an initial correction factor for the PEG/hexanol system (discussed above), it is possible that smaller additional effects on individual residues with increasing percent PEG/hexanol were not accounted for. Therefore, this could give rise to additional error in measurement of the peaks and increase the rmsd between $\Delta\delta_N$(meas) and $\Delta\delta_N$(calc). However, the applied correction from 0 to 1% most likely accounts for the majority of solvent effect because only a small percentage of the PEG/hexanol is soluble in the isotropic buffer and increasing the amount induces the formation of the liquid crystal phase. Comparison of the rmsd values between $\Delta\delta_N$(meas) and $\Delta\delta_N$(calc) for the bicelle and corrected 8% PEG/hexanol data confirms this hypothesis in that only a slight increase in rmsd is observed for alignment in PEG/hexanol (+3.9 ppb). This conclusion is also valid for $\Delta\delta_N$(meas) and $\Delta\delta_N$(calc) rmsd comparison between phage and bicelles (+4.2 ppb). Therefore, under the valid assumption that there is no solvent effect that arises from alignment in bicelles, we can rule out a significant uncorrected solvent effect on the $\Delta\delta_N$(meas) for ubiquitin aligned with 8% PEG/hexanol and Pf1 phage.

Structural effect

To investigate the effect of possible structural noise on $\Delta\delta_N$(meas), we superimposed the backbone atoms of the 1.8 Å X-ray crystal structure (Vijaykumar et al., 1987) onto the NMR structure (0.45 Å pairwise rmsd) and compared the $\Delta\delta_N$(meas) and $\Delta\delta_N$(calc) rmsds between the X-ray and NMR structures. As can be seen in Table 2, the differences between the rmsds of the X-ray and NMR structures, independent of the alignment, are approximately the same with the NMR structures producing less scatter. Thus, the $\Delta\delta_N$ data are consistent as measured by their agreement to the NMR structure. The least scatter is derived from the bicelle structures. This is intuitive since the original NMR structure was determined using phospholipid bicelles to obtain the D_{NH} used for refinement. Together, these results indicate that no matter which alignment is used, the ^{15}N CSA data fit better to the NMR solution structures with no more deviation among them than that observed between the NMR and X-ray structure, which at 0.45 Å is very small. Therefore, structural noise is not a significant source of error for any of the conditions used in these investigations.

Interestingly, residue I30 has distinct ^{15}N CSA tensor components in comparison to other residues in the helix. The $\Delta\delta_N$ values for this residue are comparable to other residues in the helix for all alignment media (Figure 1). Similarly, the D_{NH} values for I30 are within the range of RDCs observed for the residues in the helix. The difference is therefore attributed to a unique projection of the local CSA tensor onto the alignment frames. This is due to the compounded effects of having a smaller than average H^N–N–C bond angle and a ϕ dihedral value about 5° smaller than the average for the helix and is a good illustration that even a small change in local geometry can lead to a large variation in the ^{15}N CSA tensor components.

Table 2. $\Delta\delta_N$(meas) and $\Delta\delta_N$(calc) rmsd values for ubiquitin determined either by NMR or X-ray and oriented according to the alignment tensor determined for each medium

Correlation	RMSD (ppb)[a]
PEG/hexanol	
NMR	21.5 (19.0)
X_ray	24.3
Phage	
NMR	19.5 (18.7)
X-ray	24.5
Bicelles	
NMR	14.8
X-ray	18.7

[a] Numbers in parenthesis are the rmsd values after the removal of residues with internal motion or conformational exchange (see text).

Relaxation effect

It is known that dynamic properties can affect the magnitude and orientation of the ^{15}N CSA tensor by way of relaxation (Tjandra et al., 1996; Fushman et al., 1998; Fushman et al., 1999). More significantly, variation in local motion can affect each ^{15}N CSA tensor by proportional amounts. For fast motion, the contribution of dynamics is incorporated into the tensor as a function of the generalized order parameter, *S*, through the scaling of the alignment tensor. By using the previously published order parameters and discarding those few residues that were shown to have fast internal motion or chemical exchange (Tjandra et al., 1995), we can obtain an approximation for the variation in S for the residues used in the analysis. The percent deviation from the average, $\langle S \rangle = 0.845$, for these residues is only 6%. Assuming axial symmetric motion and that there are no low frequency motions with large amplitude, which are unexpected for ubiquitin based on previous relaxation studies (Tjandra et al., 1996; Fushman et al., 1998; Fushman et al., 1999), the variation about the order parameter S is so small that it is safe to conclude there is little to no differential effect of dynamics on the ^{15}N CSA tensor.

By eliminating the possibility of effects on the ^{15}N CSA tensor components by solvent, structure, or relaxation differences, we conclude that the deviations observed most likely arise from either local real variations in the tensor, or some other as of yet unincorporated variable.

Residue specific variation in σ

Variations in ϕ and ψ angles (Figure 5) coincide with individual deviations of σ_{11}, σ_{22}, σ_{33}, and β from the average values (Figure 4). The standard deviations for helical residue ϕ and ψ angles are 4.8° and 3.6° respectively, while the standard deviations for strand or extended residues are

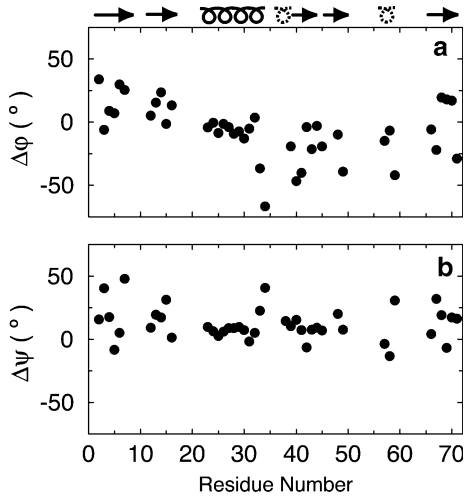

Figure 5. Deviation of ϕ and ψ from the optimal Ramachandran angles for ubiquitin as calculated from the high-resolution NMR structure.

14.4° and 14.3° respectively. Thus, our experimental data support the previous conclusions that the components of the ^{15}N CSA tensor are sensitive to local backbone configuration. These contributions obviously cannot be evaluated if it is assumed that all atoms of given type have the same tensor composition.

Many other aspects of the impact of local structural variations on the ^{15}N CSA tensor besides torsion angles were also investigated including: J coupling, hydrogen bonding, and primary or secondary shift in C, N, or H^N (Wishart et al., 1992). Plots of two of these possible contributors, H^N secondary shift and hydrogen bond energy, to individual components of the ^{15}N CSA are shown in Figure 6. Excluding the indicated residues, linear regression analysis of the H^N secondary shift (panel a) shows a possible decreasing trend in σ_{22}, however, the *r*-factor of 0.43 is so low due to scatter that it is impossible to conclude that a correlation actually exists. Nevertheless, if the correlation is present and since the secondary H^N shift is sensitive to hydrogen bonding, then a similar trend would be expected for the hydrogen bond. However, no such conclusion can be deduced from the hydrogen bond data (panel b). Even though evaluation of the extremes in hydrogen bond energy would suggest a possible increasing trend in σ_{11}, the scatter is too large to construe a definitive dependence. This uncertainty is not surprising since many factors contribute to

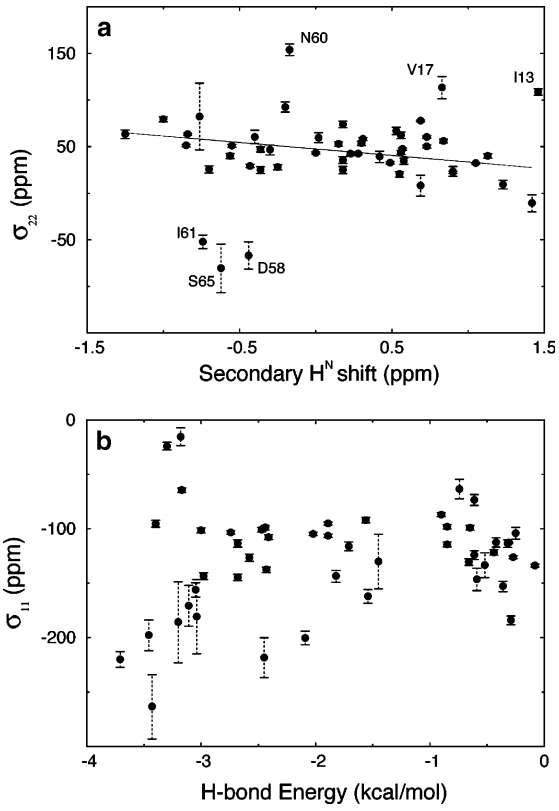

Figure 6. Plot showing the relationship between the H^N secondary shift and σ_{22} (a) and between the hydrogen bond energy (calculated using DSSP) (Kabsch and Sander, 1983) and σ_{11} (b). The outliers indicated in panel (a) were removed for linear regression analysis, which yielded an *r* factor of 0.43.

the magnitude and orientation of each component of the ^{15}N CSA tensor. Any possible trends could therefore be obscured by nearest neighbor effects, long-range interactions or other factors that cannot currently be taken into account.

Concluding remarks

The residue-specific values for the principal components of the ^{15}N CSA tensor have been determined for the protein ubiquitin utilizing three different alignment media. From these data, we have been able to gain insight into the dispersion of the tensor components, σ_{11}, σ_{22}, and σ_{33}, about the average as well as a qualitative view of the magnitude and specificity of some factors that influence the tensor, such as solvent, structure, and dynamics.

Although no strong correlation between any of the individual components of the tensor and such factors as J coupling, hydrogen bonding, primary or secondary shift in N or H^N, or dihedral angles was directly detected, several general trends have been observed that correlate well with our experimental data and previously recorded data.

Deviations from the previously determined average values are smaller than, but coincide with, previous data (Fushman et al., 1998) and are larger for residues in β-strand or extended regions, while α-helical residue tensor components cluster close to the average values. Therefore, for most α-helical residues, it is reasonably safe to assume that all residues have the same principal component magnitudes and orientations. However, for β-strand or extended segments, or residues close to the termini this assumption is less valid. Torsion angles seem to be the strongest influencing factor affecting the ^{15}N CSA tensor components in that large variance in the torsion angles also gives rise to large variance in all of the principal components. Of these, σ_{22} is affected slightly less by changes in torsion angle. At the same time, σ_{11} and σ_{22} appear to be affected by changes in the amide hydrogen environment. These results demonstrate that different factors affect the individual components of the ^{15}N CSA tensor in different ways and to different extents.

The results reported here illustrate the complexity and interdependency of factors that influence the ^{15}N CSA. Identification of possible trends in the data also suggests that were one able to differentiate among individual influencing factors, correlations between diverse physical properties, such as hydrogen bond length/angle and amide proton shifts, with the magnitude of the ^{15}N CSA principal components could be detected. Currently, however, these interactions are many and convoluted and we observe only possible trends at this time.

Acknowledgments

This work was supported by the Intramural Research Program of the NIH, National Heart, Lung, and Blood Institute.

Electronic Supplementary Material is available to authorised users in the online version of this article at http://www.dx.doi.org/10.1007/s10858-006-9037-6.

References

Barrientos, L.G., Dolan, C. and Gronenborn, A.M. (2000) *J. Biomol. NMR*, **16**, 329–337.
Bax, A. and Grishaev, A. (2005) *Curr. Opin. Struct. Biol.*, **15**, 563–570.
Braun, D., Wider, G. and Wuthrich, K. (1994) *J. Am. Chem. Soc.*, **116**, 8466–8469.
Brutscher, B., Skrynnikov, N.R., Bremi, T., Bruschweiler, R. and Ernst, R.R. (1998) *J. Mag. Resonance*, **130**, 346–351.
Case, D.A. (1998) *Curr. Opin. Struct. Biol.*, **8**, 624–630.
Chiarparin, E., Pelupessy, P., Ghose, R. and Bodenhausen, G. (2000) *J. Am. Chem. Soc.*, **122**, 1758–1761.
Cornilescu, G. and Bax, A. (2000) *J. Am. Chem. Soc.*, **122**, 10143–10154.
Cornilescu, G., Delaglio, F. and Bax, A. (1999) *J. Biomol. NMR*, **13**, 289–302.
Cornilescu, G., Marquardt, J.L., Ottiger, M. and Bax, A. (1998) *J. Am. Chem. Soc.*, **120**, 6836–6837.
De Alba, E. and Tjandra, N. (2002) *Prog. Nuclear Mag. Resonance Spectrosc.*, **40**, 175–197.
Delaglio, F., Grzesiek, S., Vuister, G.W., Zhu, G., Pfeifer, J. and Bax, A. (1995) *J. Biomol. NMR*, **6**, 277–293.
Feng, X., Eden, M., Brinkmann, A., Luthman, H., Eriksson, L., Graslund, A., Antzutkin, O.N. and Levitt, M.H. (1997) *J. Am. Chem. Soc.*, **119**, 12006–12007.
Fischer, M.W.F., Majumdar, A. and Zuiderweg, E.R.P. (1998a) *Prog. Nuclear Mag. Resonance Spectrosc.*, **33**, 207–272.
Fischer, M.W.F., Zeng, L., Majumdar, A. and Zuiderweg, E.R.P. (1998b) *Proc. Nat. Acad. Sci. USA*, **95**, 8016–8019.
Fu, R.Q. and Cross, T.A. (1999) *Ann. Rev. Biophys. Biomol. Struct.*, **28**, 235–268.
Fushman, D., Tjandra, N. and Cowburn, D. (1998) *J. Am. Chem. Soc.*, **120**, 10947–10952.
Fushman, D., Tjandra, N. and Cowburn, D. (1999) *J. Am. Chem. Soc.*, **121**, 8577–8582.
Garrett, D.S., Powers, R., Gronenborn, A.M. and Clore, G.M. (1991) *J. Mag. Resonance*, **95**, 214–220.
Harbison, G.S., Jelinski, L.W., Stark, R.E., Torchia, D.A., Herzfeld, J. and Griffin, R.G. (1984) *J. Mag. Resonance*, **60**, 79–82.
Hartzell, C.J., Whitfield, M., Oas, T.G. and Drobny, G.P. (1987) *J. Am. Chem. Soc.*, **109**, 5966–5969.
Hiyama, Y., Niu, C.H., Silverton, J.V., Bavoso, A. and Torchia, D.A. (1988) *J. Am. Chem. Soc.*, **110**, 2378–2383.
Ishii, Y., Markus, M.A. and Tycko, R. (2001) *J. Biomol. NMR*, **21**, 141–151.
Ishii, Y. and Tycko, R. (2000) *J. Am. Chem. Soc.*, **122**, 1443–1455.
Kabsch, W. and Sander, C. (1983) *Biopolymers*, **22**, 2577–2637.
Ketchem, R.R., Lee, K.C., Huo, S. and Cross, T.A. (1996) *J. Biomol. NMR*, **8**, 1–14.
Koradi, R., Billeter, M. and Wuthrich, K. (1996) *J. Mol. Graphics*, **14**, 51–55.
Kroenke, C.D., Rance, M. and Palmer, A.G. (1999) *J. Am. Chem. Soc.*, **121**, 10119–10125.
Le, H.B. and Oldfield, E. (1994) *J. Biomol. NMR*, **4**, 341–348.
Lienin, S.F., Bremi, T., Brutscher, B., Bruschweiler, R. and Ernst, R.R. (1998) *J. Am. Chem. Soc.*, **120**, 9870–9879.
Lipsitz, R.S. and Tjandra, N. (2001) *J. Am. Chem. Soc.*, **123**, 11065–11066.
Long, H.W. and Tycko, R. (1998) *J. Am. Chem. Soc.*, **120**, 7039–7048.

Lumsden, M.D., Wasylishen, R.E., Eichele, K., Schindler, M., Penner, G.H., Power, W.P. and Curtis, R.D. (1994) *J. Am. Chem. Soc.*, **116**, 1403–1413.
Mai, W., Hu, W., Wang, C. and Cross, T.A. (1993) *Protein Sci.*, **2**, 532–542.
Marassi, F.M., Ma, C., Gesell, J.J. and Opella, S.J. (1999) *Appl. Mag. Resonance*, **17**, 433–447.
Marassi, F.M. and Opella, S.J. (1998) *Curr. Opin. Struct. Biol.*, **8**, 640–648.
Oas, T.G., Hartzell, C.J., Dahlquist, F.W. and Drobny, G.P. (1987) *J. Am. Chem. Soc.*, **109**, 5962–5966.
Oldfield, E. (1995) *J. Biomol. NMR*, **5**, 217–225.
Ottiger, M., Delaglio, F. and Bax, A. (1998) *J. Mag. Resonance*, **131**, 373–378.
Palmer, A.G., Williams, J. and Mcdermott, A. (1996) *J. Phys. Chem.*, **100**, 13293–13310.
Pervushin, K., Riek, R., Wider, G. and Wuthrich, K. (1997) *Proc. Nat. Acad. Sci. USA*, **94**, 12366–12371.
Prestegard, J.H., Bougault, C.M. and Kishore, A.I. (2004) *Chem. Rev.*, **104**, 3519–3540.
Reif, B., Hennig, M. and Griesinger, C. (1997) *Science*, **276**, 1230–1233.
Reif, B., Steinhagen, H., Junker, B., Reggelin, M. and Griesinger, C. (1998) *Angewandte Chemie-International Edition*, **37**, 1903–1906.
Ruckert, M. and Otting, G. (2000) *J. Am. Chem. Soc.*, **122**, 7793–7797.
Salzmann, M., Wider, G., Pervushin, K., Senn, H. and Wuthrich, K. (1999) *J. Am. Chem. Soc.*, **121**, 844–848.
Scheurer, C., Skrynnikov, N.R., Lienin, S.F., Straus, S.K., Bruschweiler, R. and Ernst, R.R. (1999) *J. Am. Chem. Soc.*, **121**, 4242–4251.
Sitkoff, D. and Case, D.A. (1998)Theories of chemical shift anisotropies in proteins and nucleic acids *Prog. Nuclear Mag. Resonance Spectrosc.*, **32**, 165–190.
Tjandra, N. and Bax, A. (1997) *J. Am. Chem. Soc.*, **119**, 8076–8082.
Tjandra, N., Feller, S.E., Pastor, R.W. and Bax, A. (1995) *J. Am. Chem. Soc.*, **117**, 12562–12566.
Tjandra, N., Szabo, A. and Bax, A. (1996) *J. Am. Chem. Soc.*, **118**, 6986–6991.
Vijaykumar, S., Bugg, C.E. and Cook, W.J. (1987) *J. Mol. Biol.*, **194**, 531–544.
Wishart, D.S. and Sykes, B.D. (1994) *J. Biomol. NMR*, **4**, 171–180.
Wishart, D.S., Sykes, B.D. and Richards, F.M. (1992) *Biochemistry*, **31**, 1647–1651.
Xu, X.P. and Case, D.A. (2002) *Biopolymers*, **65**, 408–423.
Yang, D.W. and Kay, L.E. (1998) *J. Am. Chem. Soc.*, **120**, 9880–9887.
Yang, D.W. and Kay, L.E. (1999) *J. Am. Chem. Soc.*, **121**, 2571–2575.